Soft Matter

Cite this: *Soft Matter*, 2011, **7**, 1532

www.rsc.org/softmatter

PAPER

Polymersomes: smart vesicles of tunable rigidity and permeability

Ruddi Rodríguez-García,[a] Michael Mell,[a] Ivan López-Montero,[a] Jeanette Netzel,[ab] Thomas Hellweg[c] and Francisco Monroy*[a]

Received 15th August 2010, Accepted 30th November 2010
DOI: 10.1039/c0sm00823k

We report an experimental study on the mechanical and permeability properties of giant polymersomes made of diblock (PBD–PEO) and triblock (PEO–PPO–PEO) copolymers. These polymer amphiphiles bear the architecture and macromolecular dimensions adequate for assembling stable flat bilayers with a different hydrophobicity. In the highly hydrophobic case (PBD–PEO) an extremely compact membrane is formed, resulting in rigid polymersomes which represent a permeability barrier against solute transport across. In the case of water soluble PEO–PPO–PEO triblock copolymers, the bilayer structure is less stable in favour of the micellar state; therefore giant vesicles can be solely formed at large PPO contents. These cases (Pluronics® L121 and its mixtures with P85 and P105) are characterised by a much lower chain entangling than highly hydrophobic membranes, their polymersomes being softer than those based on PBD–PEO. Pluronic-based polymersomes are also found to be highly permeable to hydrophilic solutes, even remaining undamaged in the case of an extreme osmotic shock. This high permeability together with their high flexibility endows Pluronics polymersomes smart core/shell properties ideal to catch large biomolecules inside and able to resist under osmotic and mechanical stresses.

Introduction

Polymeric vesicles, usually referred to as polymersomes, represent a new class of vesicles made of amphiphilic block copolymers.[1–4] Polymersomes are inspired, so structurally similar, to liposomes formed from lipids. However, compared to natural liposomes, they exhibit increased mechanical stability and reduced permeability providing an impermeable physical barrier able to isolate the encapsulated material from the environment. Polymersomes have attracted enormous interest as carriers in medicine and biotechnology. Their discovery, 10 years ago, supposed indeed a conceptual advance in bioencapsulation as new membrane properties could be selected by-design. Similar to usual drug carriers based on liposomes coated by polyethylene glycol, polymersomes can be also made invisible to the immune system if made of glycol polyethers.[5–7] Furthermore, the use of synthetic polymers enables the implementation of novel membrane characteristics, opening new possibilities to enhance performances such as mechanical stability, permeability, and release rate, among others. Indeed, the therapeutic efficacy of a drug delivery system can be significantly enhanced if the content release could be triggered by a controlled stimulus. Thus, much effort has been directed to the development of stimuli-responding polymersomes useful as programmable delivery systems.

Most of these developments consider the polymer shell with a twofold function as a passive substrate for bearing the active component and as a device for programmable release. Nevertheless, despite of its massive cargo capacity, comparatively less attention has been devoted to the polymersome core as a carrier system susceptible to perform strong release by tuning shell permeability. New potential uses of polymersomes as vesicle carriers require thus a more permeable membrane enabling the possibility for core/shell transport. Further, a high permeability to hydrophilic solutes might endow an unusual resistance against osmotic shock. Increasing membrane permeability necessarily requires low core hydrophobicity and low chain entangling within, which could yet compromise stability. Therefore, fundamental studies on the structural relations existing between polymersome stability, membrane rigidity and membrane permeability are still relevant.

In this article, we report an experimental comparison between the mechanical properties of classical polymersomes made of highly dissimilar diblock copolymers and a new class based on the well-known soluble triblock poloxamers. These polymers, also known by the trade name Pluronics®, are non-ionic triblock

[a]*Mechanics of Biological Membranes and Biorheology, Departamento de Quimica Fisica I, Universidad Complutense, E-28040 Madrid, Spain. E-mail: ruddi@quim.ucm.es; ivanlopez@quim.ucm.es; monroy@quim.ucm.es; Fax: +34 91 394 4135; Tel: +34 91 394 4128*
[b]*Universität Bayreuth, Laboratory of Crystallography, Universitätsstrasse 30, D-95447 Bayreuth, Germany. E-mail: jeanette.netzel@uni-bayreuth.de; Fax: + 49 (0)921-55-3770; Tel: +49 (0)921-55-3895*
[c]*Universität Bielefeld, Fakultät f. Chemie, Physikalische und Biophysikalische Chemie, Universitätsstr. 25, 33615 Bielefeld, Germany. E-mail: thomas.hellweg@uni-bielefeld.de; Fax: +49 5211062981; Tel: +49 5211066888*

copolymers composed of a central hydrophobic chain of polyoxypropylene (PPO) flanked by two hydrophilic chains of polyoxyethylene (PEO). Poloxamer PEP–PPO–PEO membranes are relatively hydrophilic, thus less stable than those made of highly hydrophobic copolymers, subsequently only small vesicles have been obtained by soft hydration[8] extrusion[9,10] and microfluidic methods. Giant vesicles from Pluronics have been only obtained from phase reversion or emulsion methods which involve the use of organic solvents that could remain eventually trapped within the polymersome structure. To our best knowledge, we report in this article the first construction of giant polymersomes of poloxamers by the electroformation method, so opening a promising preparative way for systematic studies on these structures.

Materials and methods

Chemicals

Diblock copolymers (poly(butadiene-*co*-ethyleneoxide); PBD–PEO) with a minimal polydispersity ($M_w/M_n < 1.05$) were from Polymer Source (Canada). Pluronics L121 and F68 were from Sigma-Aldrich and P105 and P85 from BTC BASF (Belgium). The solvents and the fluorescent dyes (calcein and rhodamine) were from Sigma.

Giant unilamellar vesicles (GUVs)

Two different electroformation protocols were used to form GUVs of the studied polymersomes. The first method is an adaptation by Dimova *et al.*,[4] of the original protocol designed by Discher *et al.*,[1] for polymersome electroswelling from highly hydrophobic copolymers. The polymer is first dissolved in chloroform (2 mg mL^{-1}), then six small droplets are spread on the conductive side of an ITO-covered slide. After solvent removal in a vacuum chamber, the ITO chamber is sealed and the electrodes are connected to an AC power supply at a voltage of 5 V at 10 Hz for 1 hour. Then the chamber is filled up with the aqueous solvent containing sucrose (200 mM). Then, the voltage is slowly raised up to 9 V during 10 min and later maintained for 1 hour more. After this time a small aliquot is transferred to a glucose solution (220 mM) being then ready for phase contrast observation under the bright field mode. The second method is an adaptation well suited for Pluronics. ITO plates are connected to 5 V at 10 Hz for 2 hours. Then, the frequency is decreased down to 5 Hz and the voltage maintained at 5 V for 30 min.[11]

Fluorescence permeability assays

To evaluate the permeability of polymersomes, we have performed a commonly used technique based on the permeation of entrapped fluorescent molecules across the polymer bilayer membrane.[12] Giant polymersomes were prepared as described above adding 1 μL of the dye rhodamine or calcein dissolved in water (1 mg mL^{-1}). Then, the dyed vesicle filled with the sucrose solution was diluted (1/100) in a glucose solution (220 mM). By this procedure, the fluorescence intensity from outer vesicle fluorophores was drastically reduced. Fluorescence images are visualized by an inverted microscope (Nikon Eclipse TE2000-U, objective oil-immersion 60×). The time evolution of the change in fluorescence emission from inside the vesicles, due to dye release, was monitored with the same microscope equipped with a conventional fluorescent Hg lamp (100 W) and with a set of filters adapted to the absorption and emission wavelengths of both fluorescent dyes.

Osmotic shock experiments

Vesicles formed in sucrose solution (200 mM) were diluted (v/2) in glucose solution (220 mM). Spherical tensioned vesicles are chosen and 10 μL of buffer solution 500 mOsM (glucose 210 mM, HEPES 10 mM, NaCl, 140 mM) is added in the near vicinity of the observed vesicle. Then, vesicle evolution is followed under phase contrast microscopy.

Flickering spectroscopy

Thermal fluctuations of a single bilayer in a quasi-spherical GUV are tracked by fast CCD microscopy in the phase contrast mode (Nikon TE2000-U inverted microscope). The method, extensively described elsewhere,[13,14] is specially suited to measure bending properties. Briefly, the curvature fluctuations are described in Fourier series at the equatorial plane and the average amplitudes of the Fourier modes compared with the classical Helfrich spectrum for thermal bending modes, $P(q) = \langle u_q^2 \rangle = k_BT/(\sigma q^2 + \kappa q^4)$, obtained as a time average of the quadratic fluctuations ($\langle\,\rangle$'s are calculated over 1000 consecutive images taken at 14 fps; σ is the membrane tension, κ the bending stiffness and q the wavevector). At q sufficiently large, $q \approx 2/R$ ($>\sigma/\kappa$), bending modes largely dominate, so when integrated over the equatorial plane, the spectrum might simply vary as $P_x(q_x) \approx k_BT/\kappa q_x^3$ (q_x is the normal component of the equatorial fluctuations). From the time series of the fluctuation amplitudes at a given q the autocorrelation function is computed as $G_q(t) = \langle u_q(t)u_q(t+\tau)\rangle$.

CryoTEM

The sample is vitrified by the method described in ref. 15 and 16. Briefly, a few microlitres of diluted vesicle suspension (1 mg mL^{-1} wt%) is placed on a bare copper TEM grid (Plano, 600 mesh). The sample is cryo-fixed by rapidly immersing into liquid ethane at its freezing point. The vitrified specimen is loaded into a cryo-transfer holder (CT3500, Gatan, Munich, Germany) and transferred to a Zeiss EM922 EF-TEM (Zeiss NTS GmbH, Oberkochen, Germany).

SAXS in lamellar phases

SAXS in lamellar phases was performed at the BM16 line at ESRF (Grenoble, France). Lamellar phases made of diblock PBD–PEO copolymers were prepared by vortexing polymer films at different degrees of hydration (from 35 to 60% water w/w). The lamellar suspension is poured into borosilicate capillaries (3 mm diam.) and left to equilibrate (1 week ageing). Scattering is collected on a MARCCD 165 detector placed at 2 m from the sample, which provided a q-range from 0.2 to 1 nm^{-1} ($q = (4\pi/\lambda)\sin\theta$ is the scattering wavevector, λ and 2θ being the incident wavelength and the scattering angle, respectively).

Langmuir monolayers

Langmuir monolayer experiments were performed in a computer controlled Langmuir balance with a maximum area of 270 cm^2 (NIMA, UK)[17] following the procedure described in ref. 18. Compression isotherms were recorded upon symmetric uniaxial compression from a diluted monolayer state at a constant compression rate of 10 cm^2 min^{-1}.

Results and discussion

Diblock, *highly hydrophobic*, copolymers: high rigidity

Vesicle formation and stability. The ability of PBD–PEO diblock copolymers to form stable GUVs by electroformation was tested for three different samples with different block sizes but a similar amphiphilic character characterised by the HLB factor and the hydrophilic fraction f (see Table 1). Large unilamellar vesicles (LUVs; 200 nm radius) were also prepared by the extrusion method and its stability checked by dynamic light scattering (DLS).

The OB1 copolymer with a large PEO moiety compared to the hydrophobic PBD tail (HLB 11.1) is hydrophobic enough to form micelles ($f = 0.54$; cone aspect),[19] but unable to assemble as flat bilayers ($f < 0.45$; cylinders).[19] The copolymer OB2 with a relatively low molecular weight and relatively low hydrophilicity (HLB 6.8) is compatible with a cylindrical aspect ($f = 0.33$),[1] thus able to form stable giant vesicles by the electroformation method (see GUVs in Fig. 1) and large vesicles by extrusion (see LUVs in Fig. 2), as expected. Although OB3 has a similar aspect ($f = 0.36$) to OB2 and a relatively low hydrophilicity (HBL 7.5) in theory sufficiently low to form bilayers, it is unable to form GUVs. The PBD counterpart is in this case probably too hydrophobic, so causing this block to collapse into a denser conformation not able to form bilayers enough flat to form stable GUVs. However, OB3 bilayers might adapt the higher curvatures involved in submicron vesicle aggregates. Indeed, we have prepared LUVs made of OB3 copolymer (200 nm radius) by the extrusion method. These vesicles (OB2/OB3) remain stable for days, as revealed by DLS (the distribution of vesicle sizes was found narrow and stable for days; data not shown). Polymersome stability has been extensively checked for these polymers at similar conditions.[1,2,19,20] The giant polymersomes obtained from OB2 copolymer (typically, 10–20 μm sized) are shown in Fig. 1 as observed under contrast phase microscopy. Two unusual features characterise these polymer vesicles with respect to typical lipid GUVs: (a) a very dense membrane (observed darker than for lipid vesicles) and (b) a large amount of excess area (a number of vesicles are formed at the ellipsoidal oblate geometry) (see Fig. 1). The hydrophobic blocks strongly entangle at the membrane core, thus forming a denser shell than in lipid bilayers, which endows polymersomes with an enhanced mechanical stability.[1,2,20] Lipid bilayers are relatively permeable to water,[21] thus favouring lipid vesicles to osmotically equilibrate into a minimal surface spherical shape. However, polymersomes are created with a given area but retain the volume they initially enclose, thus they are usually found with a larger excess area than liposomes.

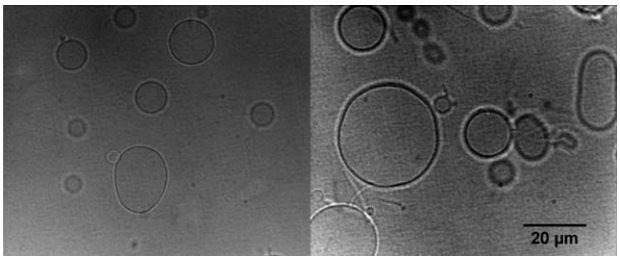

Fig. 1 Giant unilamellar vesicles of the diblock copolymer OB2 formed by the electroformation method. These polymersomes are formed predominantly unilamellar and with a large excess area.

We have also prepared small polymersomes of OB2 copolymer by the extrusion method.[22] Unilamellar vesicles are extruded through 200 nm polycarbonate membranes. Vesicles are obtained quite monodisperse, as revealed by cryoTEM (see Fig. 2). Tubular membranes, corresponding to curved micellar aggregates with a diameter similar to the vesicle thickness, are also observed in the cryoTEM images (see Fig. 2). These structures are typically found with flat bilayers in polymersome preparations.[20] Again, the vesicle membrane is observed quite dense which allows for a precise determination of the hydrophobic thickness using the contrast method described by Waninge *et al.*[23] A thickness $h = 14 \pm 1$ nm was measured for the OB2 bilayer over a population of 30 different vesicles.

Synchrotron SAXS experiments provided further insight on bilayer thickness and rigidity. Fig. 3 shows the scattering profiles obtained from the lamellar OB2 phase swollen at different hydrations. The emergence of a broad Bragg peak at decreasing water content confirms the existence of a lamellar phase made of stacks of fluctuating bilayers. Fits to the lamellar form factor[24] provide a value for bilayer thickness, $h = 13.2 \pm 0.8$ nm, almost independent of the hydration degree and in good quantitative agreement with cryoTEM estimation. Furthermore, a scaling approach,[1,2] showed relevant by molecular dynamics simulations,[25] predicts a thickness $h \approx 2aN^{0.55} \approx 14$ nm for OB2 bilayers (PBD block; polymerisation degree $N = 54$; Kuhn length $a \approx 0.8$ nm) in quantitative agreement with experiments. Lamellar diffraction peaks are actually found as a broad band centred at the characteristic lamellar distance $q_0 = 2\pi/h \approx 0.45$

Table 1 Capacity for GUV/LUV formation of the diblock copolymers used in this study (M_w is the molecular weight and $\sigma = M_w/M_n$ the polydispersity index). Amphiphilic character is characterised by the HLB factor (calculated on a molecular weight basis as 20 M_{PEO}/M_w) and the hydrophilic fraction f (calculated as a volume fraction; the respective densities are 1.13 and 1.06 g cm^{-3}, for PEO and PBD)

Polymer formula PEO_x–PBD_y	M_w/kDa	σ (M_w/M_n)	HLB	f	GUV	LUV
OB1: $x = 34$, $y = 22$	2.7	1.09	11.1	0.54	No	No
OB2: $x = 29$, $y = 46$	3.8	1.05	6.8	0.33	*Yes*	*Yes*
OB3: $x = 88$, $y = 120$	10.4	1.10	7.5	0.36	No	*Yes*

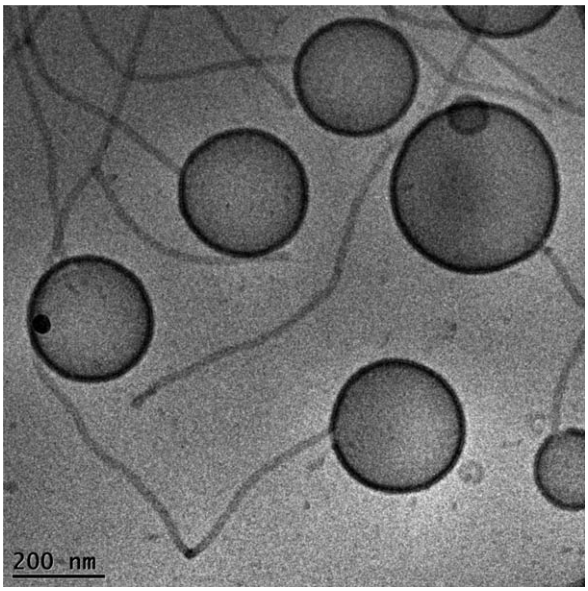

Fig. 2 CryoTEM images of the extruded OB2 polymersomes. These vesicles are formed predominantly spherical and unilamellar.

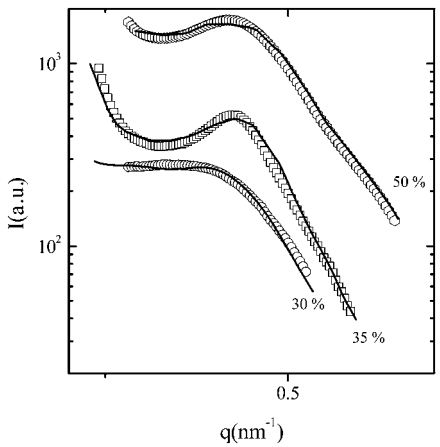

Fig. 3 SAXS profiles of OB2 lamellar phases at different hydrations (numbers indicate the polymer fraction).

nm^{-1} and with power-law decay $I(q) \approx |q - q_0|^{-\eta}$ described by the Caillé-exponent η (fitted in the $q > q_0$ range).[26] The case of extremely rigid bilayers is characterised by very sharp peaks described by high values of the exponent ($\eta \gg 1$). However, fluctuations come into play for soft bilayers and the lamellar repeat smears out. Then, Bragg peaks broaden and the Caillé parameter consequently decreases. In the present case, it is found to vary in the range $\eta = 0.08$–0.16 depending on the hydration degree (smaller values are obtained at higher hydration). These values are comparatively similar to those found for lamellar lipid phases, which are characterised by a relatively high bending stiffness ($\kappa \approx 20$–$30\ k_BT$).[27]

Membrane bending stiffness. The bending modulus of single polymersomes was measured by flickering spectroscopy. Fig. 4 shows a typical spectrum of the average curvature fluctuations registered at the equatorial plane. The data display the

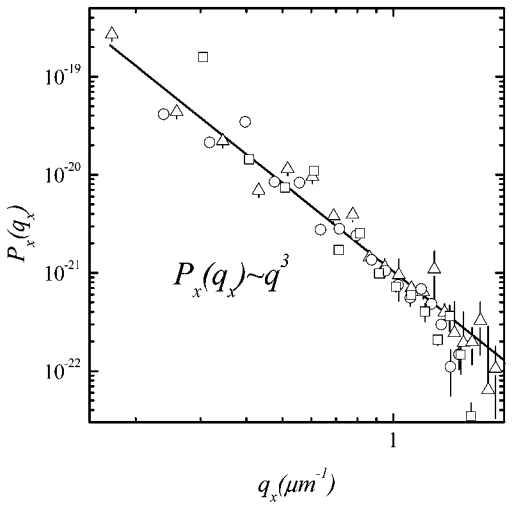

Fig. 4 Typical spectra of the shape fluctuations of giant OB2-polymersomes. Data correspond to three different vesicles. The amplitudes follow a q_x^{-3} decay (straight line), characteristic of a pure bending motion. These fluctuations are well described by the Helfrich spectrum with a bending modulus, $\kappa = 35 \pm 6\ k_BT$.

characteristic q^{-3} decay, typical for pure bending modes. No strong tension effects are detected at low q as expected for tensionless vesicles bearing large excess area ($\sigma \leq 10^{-7}$ mN m^{-1}). The best fits to the Helfrich spectrum provide a value of the bending modulus $\kappa = 35 \pm 6$ in k_BT units, calculated over a population of 15 different spherical vesicles (the error bar corresponds to the statistical variance over this population). To our best knowledge, this is the first measurement of a bending modulus of a polymersome by flickering spectroscopy, the calculated value being in quantitative agreement with previous determinations by micropipette aspiration.[1,19] Particularly, for similar polymersomes Lee *et al.*[1] have measured a bending rigidity $\kappa = 34 \pm 7\ k_BT$ and a compression modulus $K = 120 \pm 20$ mN m^{-1}. These values indicate a quite rigid system, as expected for a compact polymer layer dominated by excluded volume interactions.

Compression elasticity. As an additional piece of mechanical behaviour, we have also measured the compression modulus of OB2 monolayers as a function of lateral packing. A Langmuir monolayer of the diblock amphiphile is prepared from a chloroform solution (*ca.* 1 mg mL^{-1}) spread at the air/water interface. Fig. 5 shows the compression isotherm obtained under continuous lateral compression performed at a very slow rate to minimize dynamical effects.[28] The surface pressure isotherm ($\pi - A$) spans over more than two decades in molecular area (A), typical for polymer amphiphiles.[29] In the present case, the diblock OB2 copolymer takes two preferential conformations: (a) the flat-like state at a very large molecular area ($\pi < 10$ mN m^{-1}) and (b) a brush-like state at high pressures ($\pi > 10$ mN m^{-1}). This is the transitional conformation behavior typical for block copolymers,[30–32] the transition appearing at the collapse pressure of the hydrophilic block (in the present case, $\pi_0 \approx 10$ mN m^{-1} for PEO).[29] At surface pressures higher than π_0, the PEO block is squeezed out from the interface and a brush is formed. This

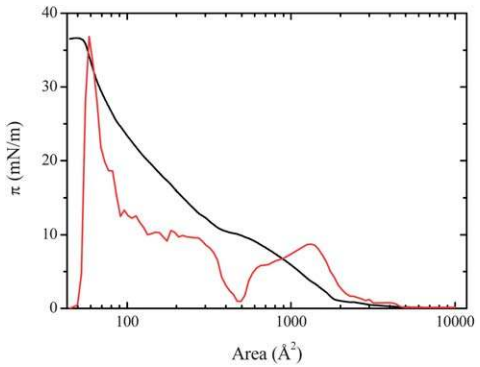

Fig. 5 $\pi - A$ compression isotherm of OB2 Langmuir monolayers (black line: 22 °C; compression rate 0.03 min^{-1}). Monolayer compression modulus ε_0 calculated as the numerical derivative of the $\pi - A$ curve (grey line).

brush-like regime is the one relevant to the bilayer polymersome state. The brush regime is dominated by entangling interactions at moderate pressure and a terminal repulsive regime at high packing. Finally, collapse is reached at a relatively high pressure ($\pi_{col} \approx 37$ mN m^{-1}) and at a low surface area ($A_{col} \approx 50$ Å^2), corresponding to the hardcore section of the normal rod (*ca.* 8 Å diameter). The compression modulus, $\varepsilon = -A(\partial\pi/\partial A)$, has been calculated as the numerical derivative of the $\pi - A$ isotherm[33] (see Fig. 5). Two maxima are observed, which correspond to optimal packing states at each monolayer regime.[29,34] One can reasonably assume the second main maxima ($\pi_{brush} \approx 32$ mN m^{-1}, $\varepsilon_{brush} \approx 38$ mN m^{-1}) as a representative of optimal packing at the brush regime ($A_{brush} \approx 65$ Å^2). This is probably the monolayer state structurally homologous to the spontaneous bilayer packing, similar to the typical molecular packing existing in lipid bilayers ($\pi_{lip} \approx 30$ mN m^{-1}, $A_{lip} \approx 60$ Å^2).[35] Israelachvili[36] has shown that optimal bilayer packing is characterized by the surface energy of the amphiphile/water interface ($\gamma \approx \pi_{brush}$), which determines the layer compression rigidity at a value $\varepsilon_{mon} = 2\gamma$ for each monolayer and twice for the bilayer $K \approx 2\varepsilon_{mon} \approx 4\gamma$.[1,36] In the present case, $\gamma \approx 32$ mN m^{-1}, the bilayer compression stiffness is expected hence to take a value $K \approx 120$–130 mN m^{-1}, in quantitative agreement with previous experimental data for similar polymersomes.[1,37] The monolayer value, $\varepsilon_{brush} \approx 38$ mN m^{-1}, is found, however, significantly lower than the theoretical prediction ($\varepsilon_{mon} = 2\gamma \approx 60$–$70$ mN m^{-1}). This difference suggests the importance of tail-to-tail interactions at the hydrophobic core of the bilayer, which are not, of course, present in the Langmuir monolayer. Furthermore, the two mechanical moduli κ and K might be mutually related; in the simplest picture, for a homogenous shell of thickness h, they might follow simple scaling,[38,39] as $\kappa = (K/\alpha)h^2$ where the denominator constant α stands for intermonolayer coupling effects (the stronger is this coupling the stiffer is the membrane). The physical meaning of the coupling constant is clear for a typical bilayer structure, like a lipid bilayer, with two well-differentiated leaflets.[39,40] At high interdigitation both monolayers are completely coupled and the membrane behaves as a homogenous rigid shell, then $\alpha = 12$. In the opposite limit, if the bilayer is supposed as two uncoupled monolayers free to slide past one another, then $\alpha \gg 12$ (lateral stresses can be released and the membrane becomes much softer). A more complex description is required in the case of a polymer membrane. In this case, additional softening could take place as a consequence of internal degrees of freedom. Consequently, an adequate description requires including chain flexibility and associated entropy,[41] thus the effective softening factor could become significantly higher than measured for lipids at free sliding ($\alpha = 48$).[40] In the present case of OB2 polymersomes, taking experimental values ($\kappa \approx 35\ k_BT$, $K \approx 2\varepsilon_{brush} \approx 70$ mN m^{-1} and $h \approx 14$ nm) one finds $\alpha \approx 95$. A similar value was obtained by Bermúdez *et al.*[37] for similar polymersomes. To summarize, these classical polymersomes are very stable structures formed by a flexible bilayer characterized by a relatively high flexural and compression rigidity, similar to classical liposomes.

Triblock, *low hydrophobicity*, Pluronic copolymers: high flexibility

Formation and vesicle stability. Triblock PEO_x–PPO_y–PEO_x Pluronics have been evidenced to exhibit a rich phase behavior in water solution depending on their relative block lengths.[42–44] The more hydrophilic copolymers with a higher water solubility (HLB > 10) associate into micellar aggregates composed of a PPO core and a PEO corona.[45] These are the cases when the copolymer hydrophilic fraction matches the structural requirement for self-assembling into curved aggregates ($f > 0.5$). On the opposite side, the more insoluble relatives with a larger PPO hydrophobic moiety have attracted less attention as they have only been predicted as a metastable state in water solution.[42,46] However, for the more hydrophobic Pluronics (HLB < 10) the bilayer condition could be fulfilled ($0.2 < f < 0.4$) thus opening the possibility for vesicle assembly in water solution. It was already envisaged by Schillen *et al.*[47] who first reported bilayer structures in diluted solutions of the hydrophobic Pluronic L121. Although a small fraction of the vesicle phase was detected in that early experiment (small LUVs with a radius *ca.* 40 nm), till recently formation of stable giant vesicles has remained elusive for these polymers. In a very recent paper, Foster *et al.*[48] have reported the first successful reconstitution of giant vesicles of Pluronic L121 by spontaneous spreading of double emulsion droplets on a water/air interface. The two surfaces on the doublet droplets are stabilised by two L121 monolayers separated by the intermediate oil phase. When the droplets touch the interface, the organic phase is expelled out and the excess surfactant exchanged with the monolayer adsorbed on. Although giant vesicles are obtained by this method, it implies complex formulation of the emulsion phase and usage of volatile organic solvents, which have risk to remain trapped within the bilayer.

In this paper, we present the first successful reconstitution of giant vesicles of hydrophobic Pluronics by the electroformation method. These giant polymersomes are quite monodisperse, predominantly unilamellar and more importantly, solvent-free, which guarantees adequate requirements for biomedical uses. We have tried several Pluronics with different hydrophobicity. Their structural characteristics and GUV-forming capacity are summarized in Table 2.

As expected, only L121, the copolymer with the lowest hydrophilic fraction (HLB 1, $f = 0.18$), is able to form stable polymersomes. Fig. 6 shows a typical L121-GUV obtained by

Table 2 Capacity for GUV formation of the Pluronics used in this study (x and y indicate block sizes). The hydrophilic fraction f is calculated as the volume fraction PEO/PPO ratio (densities $\rho_{PEO} = 1.13$, $\rho_{PPO} = 1.036$ g cm^{-3}). Three different methods for GUV formation were checked: electroformation, phase reversion[49] and soft hydration[8]

					GUV method		
Pluronics	Formula EO_x–PO_y–EO_x	M_w/kDa	HLB	f	Electrof.	Ph. revers.	Hydrat.
L121	$x = 5$; $y = 68$	4.4	1	0.18	Yes	Yes	Yes
P105	$x = 37$; $y = 58$	6.5	15	0.47	No	No	No
P85	$x = 26$; $y = 40$	4.6	16	0.47	No	No	No
F68	$x = 76$; $y = 29$	8.4	29	0.78	No	Yes?	No

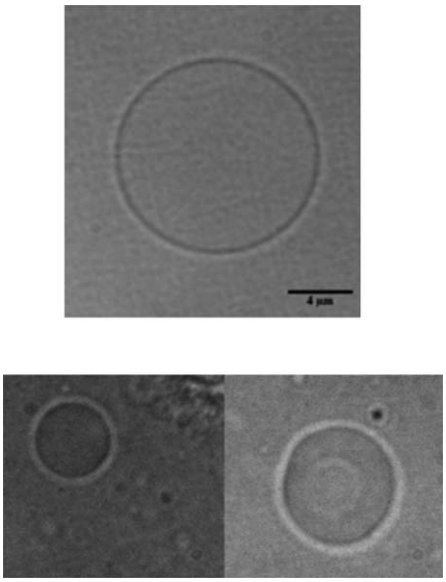

Fig. 6 (Top) GUVs of Pluronic L121 formed by the electroformation method. These polymersomes are formed predominantly unilamellar and spherical. (Bottom) Two different vesicle-like structures obtained for the non-bilayer former Pluronic F68 by the emulsion phase reversion method. Probably, they are stabilised by some organic solvents remaining trapped from the mother emulsion, so we are not certain about their vesicle character (see text for details).

electroformation and observed in the contrast phase mode. These vesicles are obtained predominantly unilamellar and, opposed to PBD–PEO diblock polymersomes, almost near spherical even under hyperosmotic conditions. Also, in comparison to diblock polymersomes, the L121 vesicles are observed with a weaker optical contrast despite the sugar used for the phase contrast observations. For L121 polymersomes the membrane is observed lighter as well. The other Pluronics studied, with the exception of F68, are unable to form giant vesicles themselves (see Table 2). These copolymers (P105 and P85) were chosen to have a similar hydrophobic moiety (responsible for membrane cohesion) and similar average molecular weight as L121. However, their absolute incapacity to form vesicles points out the importance of cylinder molecular aspect in assembling stable bilayers. Highly soluble Pluronics bearing a high PEO-content (HLB > 10) do not form GUVs in any case. Particularly interesting is, however, the case of F68, one of the more famous soluble members of the Pluronic family by its outstanding detergency properties inherent to its great ability to form micelles.[42] Despite of its marked conical aspect, due to their large PEO tails, we found giant vesicle-like aggregates formed by phase reversion (see Table 2 and bottom panel in Fig. 6). This method consists of:[52] (1) monolayer formation on oil/water emulsion droplets and (2) elimination of the organic solvent with further vesicle formation (phase reversion). Although the presence of a stabilizing polymer membrane is unequivocal (see Fig. 6), these suspicious vesicle objects display an unusual optical contrast (darkness) and a tensioned aspect (no fluctuations) invariably of the imposed osmotic gradient. This evidence strongly suggests solvent or emulsion phase trapping, thus the observed aggregates could actually consist of membrane coated solvent droplets, which puts in question this counterintuitive capacity of F68 to form vesicles. To summarize, we can conclude about a general difficulty of Pluronics to form bilayers, only the highly hydrophobic homologues (L121 among them) being adequate candidates to assemble vesicle aggregates. Next, we conduct a comparative study of the rigidity and permeability properties of L121 polymersomes with respect to the classical polymer vesicles based on the rubbery copolymer PEO–PBD.

Membrane bending stiffness. Fig. 7 shows three experimental fluctuation spectra obtained for different vesicles. Again, fluctuation amplitudes follow the characteristic q^{-3} decay typical for

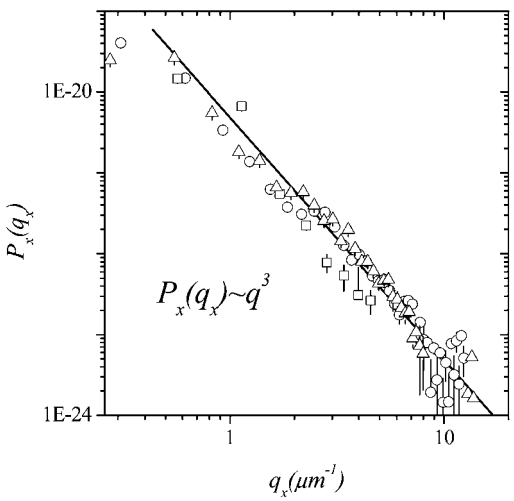

Fig. 7 Typical spectra of the shape fluctuations of giant L121-polymersomes. Data correspond to three different vesicles. The amplitudes follow a q_x^{-3} decay (straight line), characteristic of a pure bending motion. These fluctuations are well described by the Helfrich spectrum with a bending modulus, $\kappa = 3 \pm 0.6\ k_BT$.

pure bending modes at the equatorial plane. A fit to the Helfrich's law provides a value of the bending modulus $\kappa_{L121} = 1.2 \pm 0.6\ 10^{-19}$ J ($\approx 3\ k_BT$), which is much lower than found for the hydrophobic diblock copolymer ($\kappa_{PBD} \approx 35\ k_BT$), compatible with the qualitative idea of a softer membrane for L121 than for PEO–PBD. Fig. 8A shows the autocorrelation functions obtained for three consecutive Fourier modes ($q = l/R$; $l = 2, 3, 4$) in a L121 polymersome ($R \approx 4$ μm). Fittings to a mono-exponential decay law ($G_q(t) \approx e^{-\Gamma t}$) provide the q^3-dependence of the relaxation rates of the bending modes (see Fig. 8B). Milner and Safran[50] predicted the relaxation rates to vary as $\Gamma = (\kappa/4\eta)q^3$ (η being the bulk viscosity; 1.2 cP for the used buffer). This theoretical prediction is plot as a straight line in Fig. 8B (for $\kappa = 3\ k_BT$), which closely describes the experimental rates.

Compression elasticity. Fig. 9 shows the compression isotherm of L121 monolayers. Results confirm a dissimilar scenario with respect to classical diblock copolymers, a simple expanded-like regime being observed for L121. The curve, typical of soluble glycol polymers,[30] displays a monotonous increase from the diluted regime up to a collapsed pseudo-plateau. The non-horizontal plateau is characteristic of a diffuse brush produced by the progressive solubilisation of the hydrophilic blocks in the water subphase.[29,30] However, no true grafted brush is formed in this case, further monolayer compression causing the complete dissolution of the molecules in water (this is because the pseudo-plateau corresponds to a full compressibility regime; ε drops to zero there).[30] The maximal rigidity is raised at a relatively expanded state (at $A \approx 1000$ Å^2, $\pi \approx 25$ mN m^{-1} and $\varepsilon_{max} \approx 22$ mN m^{-1}), corresponding to a fuzzy packing (at this state L121 molecules conform as random coils with a cross-sectional area $A_0 = \pi R_g^2 \approx \pi a^2 N \approx$ 1000–1200 Å^2; $N \approx 73$, $a \approx$ 5–6 Å). The

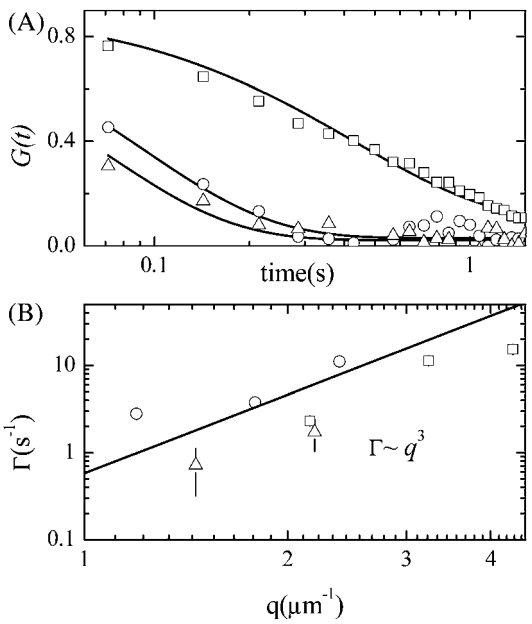

Fig. 8 (A) Experimental autocorrelation functions of the shape fluctuations of a typical giant L121 polymersome. The straight lines correspond to fits to a single exponential relaxation. (B) q-dependence of the experimental relaxation rates. (—) Theoretical prediction for $\kappa = 3\ k_BT$ (see text for details).

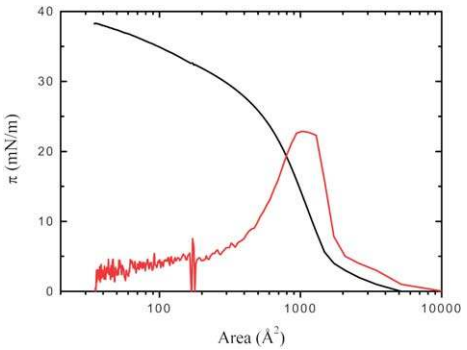

Fig. 9 $\pi - A$ compression isotherm of L121 Langmuir monolayers (black line: 22 °C; compression rate 0.03 min^{-1}). Monolayer compression modulus ε_0 calculated as the numerical derivative of the $\pi - A$ curve (grey line).

results confirm the mechanical scenario sketched above, which assigns L121 membranes a much softer character (L121: $\kappa \approx 3\ k_BT$, $K \approx 40$ mN m^{-1}) than classical diblock copolymers (OB2: $\kappa \approx 35\ k_BT$, $K \approx 120$ mN m^{-1}).

Membrane permeability

The permeability properties of the two classes of polymersomes were investigated. Giant vesicles are prepared in electroswelling buffer containing water soluble dyes (calcein and rhodamine). After GUV formation, a small aliquot (50 μL) is diluted in a dye-free equiosmolar medium (1 mL) and immediately observed under fluorescence microscopy. Two aliquots are stored in darkness (at 5 °C) for late observation one hour and two hours after dilution. As no fluorescence excitation is produced during storage, late observation is not affected by photobleaching artefacts. Fig. 10 shows typical results for preparations containing calcein. In the high hydrophobicity case (Fig. 10, top panel: OB2 PBD–PEO copolymer), vesicles are observed with a large contrast in the bright field mode (right panel), suggesting a small or zero permeability to sugars used as optical contrast enhancers. Fluorescence observation in the calcein channel shows that the fluorescent probe remains trapped inside the

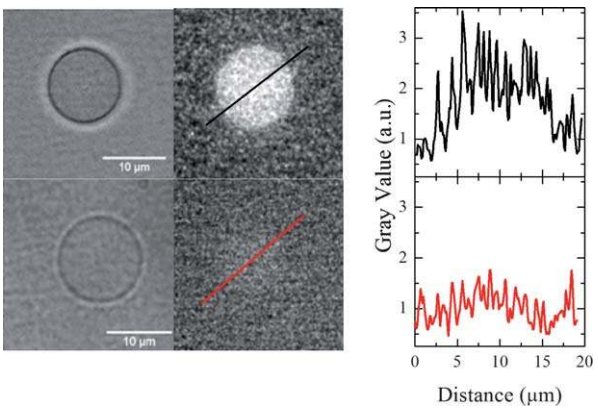

Fig. 10 Calcein permeability assays on OB2 (top) and L121 (bottom) GUV polymersomes: bright field (left images) and calcein fluorescence channel (right images). Plots correspond to the intensity profiles along the respective lines on the fluorescence images.

vesicle. A similar fluorescence intensity is recorded as a function of time, confirming the impermeable character of the PBD–PEO membrane against calcein transport. The case of L121 polymersomes is completely different (Fig. 10, bottom panel). The optical contrast is weak in the bright field mode. No fluorescence is detected immediately after dilution or in later observations (1–2 hours after preparation). In both cases, images were taken at identical exposure times thus results can be unequivocally interpreted as the diffusive loss of the calcein dye across the membrane. Fig. 11 shows an additional permeability test performed with rhodamine (slightly more hydrophobic than calcein). For diblock copolymers the membrane is again impermeable to rhodamine (fluorescence intensity is always larger inside; see Fig. 11, top panel). We observe in this case a significant accumulation of rhodamine in the membrane which suggests a certain hydrophobic affinity for the PEO-brush. On the other hand, an evident rhodamine loss is observed for L121 polymersomes (see Fig. 11, bottom panel), the inner fluorescence intensity being in this case equal to the outer background. As in the former case, rhodamine is in part retained (probably absorbed) by the polymer bilayer. A differential scenario can be sketched from these permeability tests: (a) PBD–PEO membranes constitute a permeability barrier against small solutes (dyes: calcein, rhodamine, ions and sugars) and only weakly permeable to water. (b) Contrarily, L121 membranes are highly permeable to small ions, sugars and water.

Membrane resistance to osmotic shock

To clarify these differences we have designed different experiments where the two classes of polymersomes are stressed by a massive osmotic shock (see Fig. 12). In a first series, polymersomes of the hydrophobic diblock copolymer (OB2) are exposed to: (S1.A) saline hyperosmotic medium (130 mM NaCl; Fig. 12, top) and (S1.B) sucrose/glucose gradient (Fig. 12, middle). In both cases, budding instabilities are immediately observed after osmotic shock, indicating water outflow. In an early stage, recently created excess area is stabilised as buds, which are later ejected as small daughter vesicles. In general, the higher the osmotic distress the larger the buds produced, not only

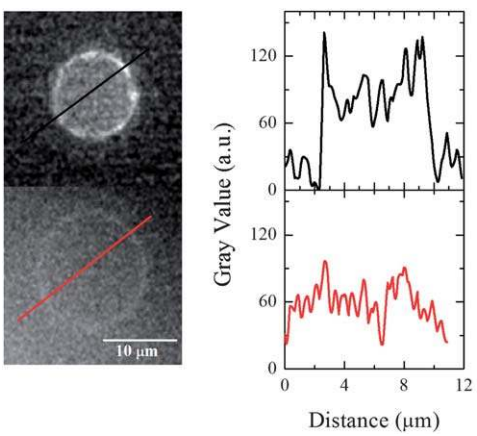

Fig. 11 Rhodamine permeability assays on OB2 (top) and L121 (bottom) GUV polymersomes. Plots correspond to the intensity profiles along the respective lines on the fluorescence images.

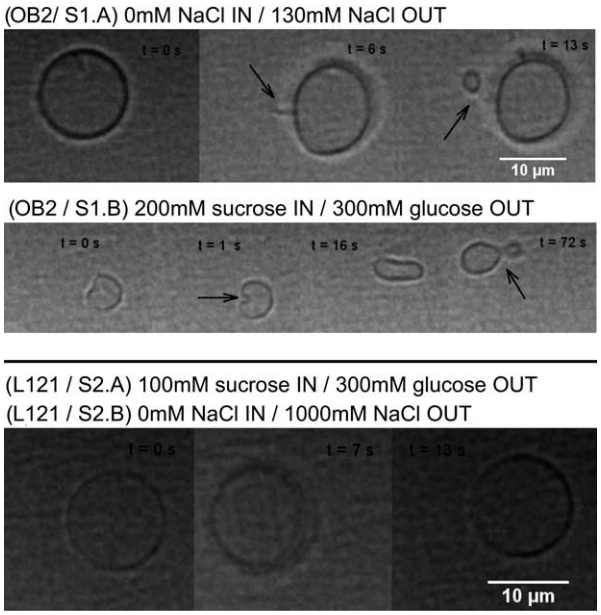

Fig. 12 Osmotic shock tests on OB2 (top) and L121 (bottom) polymersomes. See text for details.

in number but also in size. This budding response has been extensively studied in classical polymersomes.[1,2,19,20]

The case of L121 polymersomes is considered in a second series (S2; Fig. 12, bottom). In this case, vesicles were exposed to different solutes (NaCl, sucrose, glucose, …) at moderate (200 mM) and at extreme (1000 mM) concentrations. Surprisingly, despite the strength of the osmotic shock L121 polymersomes remain invariably unaltered (see Fig. 12, bottom). Even under massive water dilution (normally vesicles might explode), L121 polymersomes resist unchanged. This outstanding behaviour suggests a practically free passage of water and small solutes across the membrane even under massive osmotic shock. Hence, any osmotic gradient applied to the system is completely smeared out by *quasi*-free diffusion.

PBD–PEO *vs.* Pluronics: compactness *vs.* porosity

From the above evidence two different membrane scenarios can be sketched (see Fig. 13).

(A) PBD–PEO. The diblock architecture entails a bilayer structure where the copolymer chains assemble as two opposite tail-to-tail monolayers. High PBD-hydrophobicity endows assembling as very compact bilayers stabilised by chain entangling and monolayer interdigitation. Consequently, and this is a *state-of-the-art* conclusion, the resulting polymersomes behave relatively rigid and impermeable to hydrophilic solutes.[1,2,5,20]

(B) Pluronics. Hydrophobic Pluronics, particularly L121 and probably also other analogues, represent a new class of polymersome formers able to assemble fuzzy bilayers. Differently to amphiphilic diblocks, the triblock architecture does not impose a defined conformation for the chain in the aggregates. Both, I-shape and U-shape conformations are ambiguously preferred by the bilayer assembly (see Fig. 13, right). As PPO and PEO are

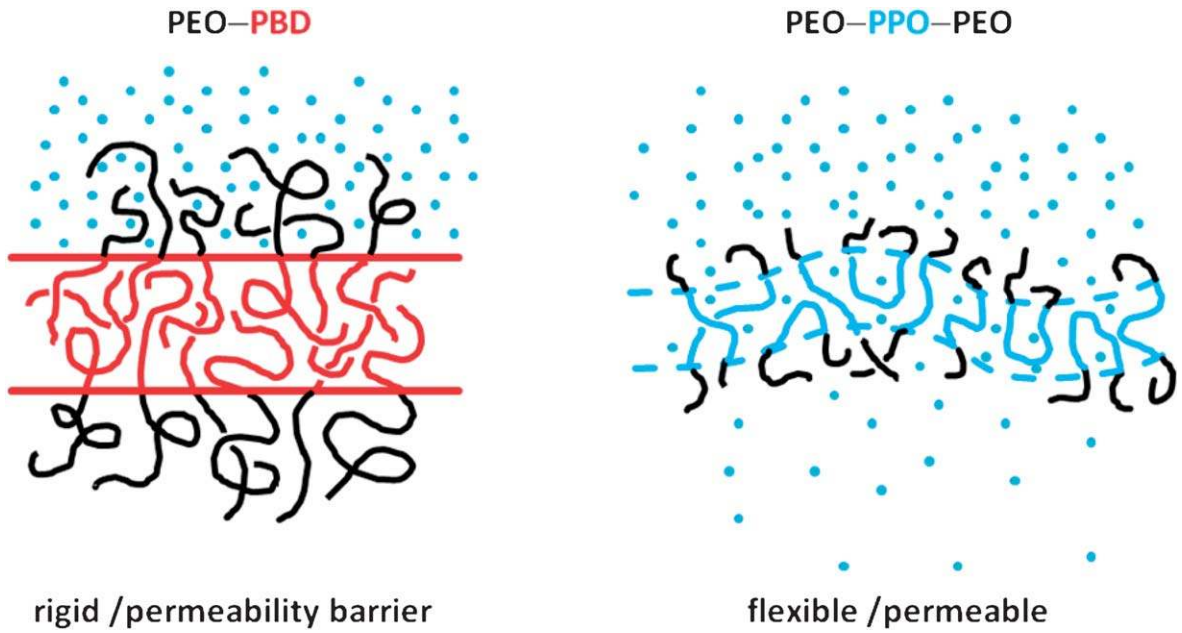

Fig. 13 Differential membrane behaviour of highly hydrophobic PBD–PEO (left) and Pluronics (right). See text for details.

mutually compatible, there is no strong spatial segregation between the two blocks. Consequently, there should be no high energy barrier for conformational interconversion, neither against intermonolayer flip–flop. Moreover, PPO is relatively soluble in water, thus one expects the membrane PPO-core swollen in a gel-like state. All these convert L121 bilayers into a very dynamic assembly with a high porosity. Consequently, and this is the original conclusion emerged from this work, the resulting Pluronics polymersomes behave like a soft porous shell, *i.e.* with a low membrane rigidity and a high permeability to hydrophilic solutes. These unusual performances convert Pluronics into excellent candidates for self-assembling membranes with a controllable permeability in giant polymersome devices.

Pluronics binary mixtures

Unfortunately, not a large repertoire of bilayer-formers is expected among the Pluronics grid (only the highest hydrophobic HLB < 10 might be suitable). Thus, polymer blending appears as a good alternative for screening structure-to-property enhancement. Compatible blending requires topological matching at the bilayer core, thus only the homologues with a similar PPO block might be adequate for vesicle formation. On this hypothesis we have checked polymersome formation for compatible blends of L121 with similar P105 and P85. F68 is too dissimilar to L121, thus no GUVs were obtained at any composition.

(A) L121 + P85. Previous to this work, using the shear-method, Netzel and Hellweg[51] have pointed out the ability of Pluronic P85 to form not only micelles but small vesicles as well ($R \approx 50$–100 nm). In that method, highly curved vesicles are forced to form from a concentrated lamellar phase strongly sheared in a rotational strain field. Probably, because of their relatively large structural symmetry ($f \approx 0.5$; see Table 2), P85 does not bear a high spontaneous curvature thus forming relatively stable bilayers with respect to highly curved micellar aggregates. Li *et al.*[52] have also discussed the stabilising role of P85 micelles on small vesicles made of L121. Using cryoTEM, they describe the mutual solubility of both structures into a binary vesicle aggregate able to mutually bunch into vesicle clusters. This stabilisation role has been checked here in giant polymersomes made of the binary system L121 + P85. Fig. 14 shows different GUV preparations from the binary system. The non-bilayer former P85 can be incorporated in polymersome formulations up to 70% weight. No vesicles are, however, encountered for L121 contents smaller than 30% (w/w), which points out the central role of L121 on the zero curvature necessary to stabilise a bilayer in a giant vesicle.

(B) L121 + P105. Although P105 has a similar hydrophilic fraction as P85, it is significantly more hydrophilic in absolute terms (larger PEO and higher M_w). Also, water solubility is also

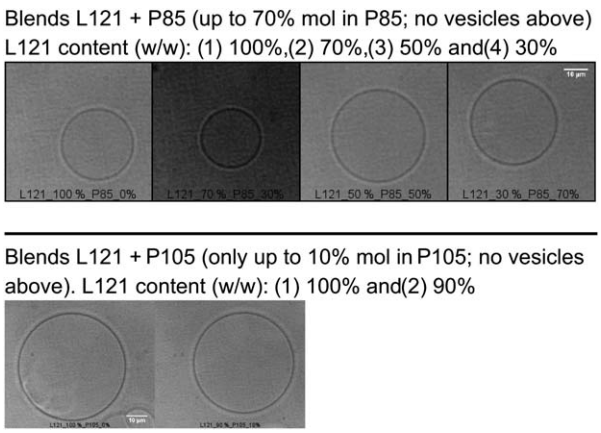

Fig. 14 Binary polymersomes of L121 blends with P85 (top) and P105 (bottom). See text for details.

higher for P105 than for P85. Consequently, even being a good candidate for blending with L121 (similar PPO moieties), P105 only forms stable vesicle up to a 10% weight fraction (see Fig. 14, bottom). Higher P105 contents completely impede vesicle formation, probably in favour of binary micelles which solubilise L121 inside. Indeed, F68 represents the limit case of competitive aggregation; being an excellent micelle former and mutually compatible with L121, they mix together to form binary micelles even at minimal F68 contents. Although blending with non-bilayer Pluronics is adequate to formulate polymersomes with enhanced properties (mainly related to the surface PEO block, adhesion, for instance), the results highlight the very important fact that a given proportion of doping agent—*progressively smaller with increasing PEO*—gives rise to a bilayer destabilisation in favour of the more stable micellar aggregate. Consequently, vesicles do not form even in the majority of bilayer formers such as L121.

Conclusions

We have determined mechanical and permeability properties of giant polymersomes based on amphiphilic diblock copolymers (PBD–PEO) and triblock Pluronics (PEO–PPO–PEO). The Pluronic family has been considered for its low hydrophobicity compared to classical block copolymers used in polymersome formulation. We report for the first time the successful electroformation of giant polymersomes based on Pluronic L121 and their blends with P105 and P85. Whereas rubbery diblock copolymers PBD–PEO build classical polymersomes (relatively rigid and permeability barrier), Pluronic L121 assembles a floppy mesh highly permeable to water and solutes. These outstanding performances convert Pluronics polymersomes into excellent candidates for assembling core/shell devices with controllable properties.

Acknowledgements

We thank ESRF for allocating SAXS beamtime at BM16. We are grateful to M. Cócera and F. Fauth for assistance with SAXS experiments and to M. Drechsler with cryoTEM. ILM thanks MICINN for a *Juan de la Cierva* contract. RRG was financed by FPI-MICINN program and MM by FPU-MICINN. JN profited a short-term stage financed by *Acciones Integradas/DAAD* program (HD2008-0051). This work was supported by MICINN (grants FIS2009-14650-C02-01, HD2008-0051 and Consolider Ingenio CSD2007-0010) and CAM (NOBIMAT S2009MAT-1507).

References

1 B. M. Discher, Y. Y. Won, D. S. Ege, J. C. Lee, F. S. Bates, D. E. Discher and D. A. Hammer, *Science*, 1999, **284**, 1143.
2 B. M. Discher, H. Bermudez, D. A. Hammer, D. E. Discher, Y.-Y. Won and F. S. Bates, *J. Phys. Chem. B*, 2002, **106**, 2848.
3 S. Belegrinou, J. Dorn, M. Kreiter, K. Kita-Tokarczyk, E. K. Sinner and W. Meier, *Soft Matter*, 2010, **6**, 179.
4 R. Dimova, U. Seifert, B. Pouligny, S. Förster and H.-G. Döbereiner, *Eur. Phys. J. E: Soft Matter Biol. Phys.*, 2002, **7**, 241.
5 P. Photos, R. Parthasarathy, B. Discher and D. E. Discher, *Book of Abstracts, 36th Middle Atlantic Regional Meeting of the American Chemical Society*, Princeton, NJ, 2003, p. 175.
6 F. Meng, G. H. M. Engbers and J. Feijen, *J. Controlled Release*, 2005, **101**, 187.
7 L. Ayres, P. Hans, J. Adams, D. W. P. M. Loewik and J. C. M. van Hest, *J. Polym. Sci., Part A: Polym. Chem.*, 2005, **43**, 6355.
8 A. T. Nikova, V. D. Gordon, G. Cristobal, M. R. Talingting, D. C. Bell, C. Evans, M. Joanicot, J. A. Zasadzinski and D. A. Weitz, *Macromolecules*, 2004, **37**, 2215–2218.
9 K. Schillen, K. Bryskhe and Y. Mel'Nikova, *Macromolecules*, 1999, **32**, 6885–6888.
10 F. Li, L. Haan, A. Marcelis, F. Leermakers, M. Stuart and E. Sudhölter, *Soft Matter*, 2009, **5**, 4042–4046.
11 M. Sauer, T. Haefele, A. Graff, C. Nardin and W. Meier, *Chem. Commun.*, 2001, 2452–2453.
12 I. Shimanouchi, U. Yoshimoto and U. Kuboi, *Colloids Surf., B*, 2009, **73**, 156.
13 J. Pécréaux, H. G. Döbereiner, J. Prost, J. F. Joanny and P. Bassereau, *Eur. Phys. J. E*, 2004, **13**, 277–290.
14 R. Rodriguez-Garcia, L. R. Arriaga, M. Mell, L. H. Moleiro, I. Lopez-Montero and F. Monroy, *Phys. Rev. Lett.*, 2009, **102**, 128101.
15 Z. Li, E. Kesselman, Y. Talmon, M. A. Hillmyer and T. P. Lodge, *Science*, 2004, **306**, 98.
16 A. Wittemann, M. Drechsler, Y. Talmon and M. Ballauff, *J. Am. Chem. Soc.*, 2005, **127**, 9688.
17 F. Grunfeld, *Rev. Sci. Instrum.*, 1993, **64**, 548.
18 L. R. Arriaga, I. Lopez-Montero, J. Ignes-Mullol and F. Monroy, *J. Phys. Chem. B*, 2010, **114**, 4509.
19 D. E. Discher and A. Eisenberg, *Science*, 2002, **297**, 967–973.
20 D. E. Discher and F. Ahmed, *Annu. Rev. Biomed. Eng.*, 2006, **8**, 323–341.
21 K. Olbrich, W. Rawicz, D. Needham and E. Evans, *Biophys. J.*, 2000, **79**, 321–327.
22 L. Mayer, M. Hope and P. Cullis, *Biochim. Biophys. Acta, Biomembr.*, 1986, **858**, 161.
23 R. Waninge, T. Nylander, M. Paulsson and B. Bergenståhl, *Colloids Surf., B*, 2003, **31**, 257–264.
24 S. Förster, A. Timmann, C. Schellbach, A. Frömsdorf, A. Kornowski, H. Weller, S. Roth and P. Lindner, *Nat. Mater.*, 2007, **6**, 888–893.
25 G. Srinivas, D. F. Discher and M. L. Klein, *Nat. Mater.*, 2004, **3**, 638.
26 A. Caillé, *C. R. Seances Acad. Sci., Ser. B*, 1972, **274**, 891.
27 G. Pabst, J. Katsaras, V. Raghunathan and M. Rappolt, *Langmuir*, 2003, **19**, 1716–1722.
28 H. Hilles, A. Maestro, F. Monroy, F. Ortega, R. Rubio and M. Velarde, *J. Chem. Phys.*, 2007, **126**, 124904.
29 D. Langevin and F. Monroy, *Curr. Opin. Colloid Interface Sci.*, 2010, **15**, 283.
30 M. Muñoz, F. Monroy, F. Ortega, R. Rubio and D. Langevin, *Langmuir*, 2000, **16**, 1083–1093.
31 S. Rivillon, M. G. Muñoz, F. Monroy, F. Ortega and R. G. Rubio, *Macromolecules*, 2003, **36**, 4068.
32 H. M. Hilles, M. Sferrazza, F. Monroy, F. Ortega and R. G. Rubio, *J. Chem. Phys.*, 2006, **125**, 074706.
33 F. Monroy, F. Ortega and R. G. Rubio, *Phys. Rev. E: Stat. Phys., Plasmas, Fluids, Relat. Interdiscip. Top.*, 1998, **58**, 7629.
34 R. Miller, L. Liggieri and V. V. Krotov, *Interfacial Rheology*, Brill, Leiden, Boston, 2009.
35 D. Marsh, *Chem. Phys. Lipids*, 2006, **144**, 146.
36 J. Israelachvili, *Intermolecular and Surface Forces*, Academic Press, London, 1992.
37 H. Bermúdez, D. A. Hammer and D. E. Discher, *Langmuir*, 2004, **20**, 540.
38 L. Landau and L. Lifshitz, *Theory of Elasticity*, Oxford, New York, 1970.
39 W. Helfrich, *Z. Naturforsch., C: J. Biosci.*, 1975, **30**, 841.
40 E. Evans, *Biophys. J.*, 1974, **14**, 923.
41 I. Szleifer, D. Kramer, A. Ben-Shaul, D. Roux and W. M. Gelbart, *Phys. Rev. Lett.*, 1988, **60**, 1966.
42 B. Chu and Z. Zhou, *Nonionic Surfactants: Polyoxyalkylene Block Copolymers*, ed. V. M. Nace, Surf. Sci. Ser. vol. 60, Marcel Dekker Inc., NY, 1996.
43 P. Alexandridis, *Curr. Opin. Colloid Interface Sci.*, 1997, **2**, 478.
44 http://www2.basf.us/performancechemical/bcperfpluronic_grid.html.

45 K. Mortensen and W. Brown, *Macromolecules*, 1993, **26**, 4128.
46 P. N. Hurter, J. M. H. M. Scheutjens and T. A. Hatton, *Macromolecules*, 1993, **26**, 5592.
47 K. Schillen, K. Bryskhe and Y. S. Mel'nikova, *Macromolecules*, 1999, **32**, 6885.
48 T. Foster, K. D. Dorfman and H. T. Davis, *Langmuir*, 2010, **26**, 9666.
49 A. Moscho, O. Orwar, D. Chiu, B. Modi and R. Zare, *Proc. Natl. Acad. Sci. U. S. A.*, 1996, **93**, 11443.
50 S. T. Milner and S. A. Safran, *Phys. Rev. A: At., Mol., Opt. Phys.*, 1987, **36**, 4371–4379.
51 J. Netzel and T. Hellweg, manuscript in preparation.
52 F. Li, L. J. de Haan, A. T. M. Marcelis, F. A. M. Leermakers, M. A. C. Stuart and E. J. R. Sudhölter, *Soft Matter*, 2009, **5**, 4042.

